



## Premature-Multiple Stage Brain Tumour Detection and Localization using a Fusion of K-Means Clustering and Patch-based Processing

Sethuram Rao G<sup>1\*</sup>, Vydeki.D<sup>2</sup>, Pavithra K<sup>3</sup>, Boomikha E<sup>4</sup>, Rahul M<sup>5</sup>, Padmanaban V<sup>6</sup>, Dhanush Shobin G<sup>7</sup>

<sup>1</sup>Assistant Professor, Velammal Institute of Technology, Chennai.

<sup>2</sup>Professor, VIT Chennai.

<sup>3,4,5,6,7</sup>Student, Velammal Institute of Technology, Chennai.

\*Corresponding author: Sethuram Rao G, Assistant Professor, Velammal Institute of Technology, Chennai, Email: sethuramvit@gmail.com

Submitted: 20 March 2023; Accepted: 16 April 2023; Published: 17 May 2023

### ABSTRACT

Brain Tumour is a significant global health issue that results in high mortality rates. Early detection and treatment are crucial for a successful patient recovery. Brain MR images are used to obtain critical tumour characteristics such as location, size, and type to accurately diagnose the disease. This study proposes an efficient approach to detect and locate brain tumours in MR images using a fusion of k-means clustering, patch-based image processing, and object counting. The experimental results conducted on 20 MR images with ground truth show that the proposed technique is capable of detecting multiple tumours despite differences in intensity level, size, and location. The simulated results of the proposed method outperform other existing techniques, with average values of precision, accuracy, specificity, and dice score of 98.48%, 99.89%, 99.99%, and 95.88%, respectively.

**Keywords:** *Magnetic Resonance Image, K-means clustering, Patch based algorithm, segmentation, Tumor*

### INTRODUCTION

Brain being the central part of the body is very sensitive and complex in nature controls the entire functionality of the body. Any damage to the brain affects the performance of the overall organs in the body very badly. Due to abnormal growth of cells a mass like structure will form, called tumour. This tumour can be benign or malignant. Benign are non-cancerous and malignant are cancerous tumour which will affect the brain and one of the leading causes of death. Hence to increase the survival of affected person automatic and accurate detection of the tumour is very crucial.

Though many approaches are available for classification and location of a tumour in human brain, still there is wide requirement for development and is always a challenging task.

MRI, CT, X-ray systems contribute to most advanced medical image modalities; out of which MR image plays vital role because of its non-invasive soft tissue contrast imaging. Hence MRI is most preferred tool for diagnosis [2] of tumour in human brain. MRI system makes use of radio waves with strong magnetic field to align the strong magnetic field

around the human body. During this process water content of brain tissue are reflected while the radio frequency is aborted resulting in signal called free induction decay (FID). A two dimensional (2D) image of the brain tissue are obtained by processing FID signal further.

MRI systems are capable of generating image of different anatomical structures like brain and other organs. From the brain anatomical structure, detailed information about brain tumour portion can be obtained such as orientation, shape location and size [3]. This information can help medical experts to diagnose tumours manually and prescribe the treatment procedure. But due to the complex nature of tumour in terms of its shape size colour and intensity manual diagnosis is always a tedious process and more time consuming task. To overcome the above limitation and make diagnosis process more accurate and reliable, automated segmentation and detection techniques are very much in need [4].

#### RELATED WORK

Preprocessing an image performs a vital role in brain image segmentation in which skull stripping is done to isolate non-cerebral tissues from the brain MR image [5, 6]. Over the year's different skull stripping techniques are developed. Hahn et al introduced one of the technique using 3D watershed combined with modified water shed algorithm. [7]. Segonne et al proposed a mixed approach for models like deformable surface with a combination of water shed algorithm [8]. Sadananthan et al demonstrated a model based on stripping of skull technique involving intensity, graph cuts and thresholding. Even though this approach is successful in procuring the brain edge, the resultant brain mask eliminates narrow connections. They have a limitation by means of complexity intensive computation, prone to over sampling and brain tissue erosion. After careful study of the entire skull stripping methods, implementation of speedy and accurate skull stripping is done by multiple thresholding and object counting in this proposed approach. Literature survey includes a variety of machine vision techniques that contributes the

development of medical image segmentation [10]. Karkinas et al approach deals with wavelet decomposition to secure the colour wavelet covariance features in an endoscopic video [11]. Logeswari et al presented hierarchical self-organizing map (SOM) by detaching noise and recognizing the principle tissue structures with a combination of Fuzzy c-means clustering [12]. Sinha et al introduced three techniques using optimized c-means clustering with generic algorithm and k-means watershed algorithm [13]. Magersa et al introduced skull stripping and fuzzy hop field neural network for tumour segmentation [14]. Bahadure et al introduced Berkley wavelet transformation and SVM to enhance process of segmentation. K Sooknanan et al started a technique using basic approaches like k-means clustering, anisotropic diffusion, morphological operations, temporal smoothing with volumetric measurement [16]. Hazra et al presented a brain tumour detection technique comprised of stages like edge detection, noise removal and k-means clustering [17]. Another approach developed by Khanat et al is to detect brain tumours which include morphological operations along with wavelet transformation and k-means clustering for segmentation and extracting tumour position respectively.

From the majority of approach presented in above literature survey, it is observed that segmentation of MR image is done by not considering the localizing of the tumour region. And hence it leads to failure of the system to detect multiple and small size tumours. Even though some of the techniques can detect a single tumour, but they fail to address the detection and localization tumours of small size and multiple tumours. In this paper the above limitations are surmounted with the help of k-means clustering to predict the neighbouring edge of the brain. Next the MR image is divided into patches which are repeatedly scaled. Finally, object detection and counting using multiple threshold values are followed. In this proposal, the novelty and contribution is that the system can be able to identify both maximum and minimum size tumours in a single MR image by not implementing modern algorithms like machine learning and deep learning.

### METHODOLOGY

In this methodology, digital image processing techniques are applied like k-means clustering, Patch based image processing, object counting and tumour estimation.

#### *k-means clustering*

K-means clustering algorithm adapts a supervised approach which mainly works on splitting the intensity levels of an image with reference to the cluster centroids. In this approach a particular pixel and its neighboring centroid distance are taken into account for calculation. The approach is implemented, such that every pixel value assigned to particular centre point which has a small distance value. Every time the centroids and pixels are reassigned the distance value is updated. This K-means cluster comes under supervised density algorithm which divides the intensities of an image based on clusters centroids. Here each image pixel and its corresponding centroid distance are calculated. The algorithm works such that each pixel value assigned to a particular centroid is based on the minimum distance value. Every time the centroids and pixels are reassigned the distance value is updated. This process is repeated till the distance of centroids and pixel will have considerable changes [16]. By making cluster variance to a minimum value the efficiency of k-means cluster can be achieved. This has been shown in equation 1 and 2. Equation 1 is achieved by minimizing sum of squares within each cluster variance (SSW).

Similarly, Sum of squares (SSB) between clusters gives maximum cluster variance as shown in equation 2.

$$SSW(C, K) = \sum_{i=1}^N \|x_i - c_k\|^2 \quad (1)$$

$$SSB(C, K) = \sum_{j=1}^N n_j \|c_j - \bar{x}\|^2 \quad (2)$$

If SSW has minimum value then higher will be the intra cluster unity value which is connected by means of the specified cluster configuration. Simultaneously, SSB has a greater value cluster configuration if there is significant degree of separation. Fig.1 gives the flow chart for k-means clustering algorithm.

#### *Patch Based Image Processing*

The prime objective of patchbased processing is to divide the input original image into patches of small size. These partitioned patches are dealt independently; latter on integrated to give the concluding processed image. These technique works well for detecting and localizing tumours of small size, rather than detecting tumour image of normal scale. Hence every patch of the original image is scaled thrice of its original size. Latter every scaled patch under goes k-means clustering object counting followed by tumour evaluation, So that each patch will be detected and localized for tumours. Finally, refined patches are merged to produce the count of the identified tumours from the original input brain MR image.

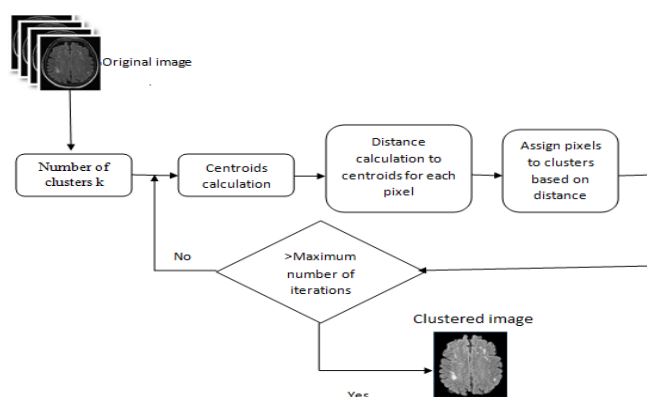


**FIG 1:** Steps used in proposed k-means algorithm

### ***Tumour Detection using Object counting***

Motive of counting technique in MR images is to locate tumour object and perform localization. A binary image composed of black and white gray value is connected with a group of pixels with high intensity is called as tumour object. Making use of thresholding technique and erosion the input MR image is transformed to numerous binary images. These images when compared with object counting till all the patches constituting of objects is considered as one image.

### ***Tumour Evaluation and Processing Steps***

Step 1: Original MR Image undergoes k-means clustering, which is divided into three regions: High intensity region which is possible tumours, medium intensity regions (cerebrum region) and dark regions as shown in figure 1 flowchart.

Step 2: Region growing and morphological skull stripping technique is used on brain image to remove the additional cerebral tissue like skin, fat and skull.

Step 3: False tumours look like which is due to the skull part remains are removed by choosing a threshold value having a Euclidean distance allying with cerebral and brain surrounding tissue.

Step 4: The original MR image is split into two. First one is archived by building a product between complemented highest neighbouring edges at the centre with average intensity value of k-means cluster. The second one is obtained by subjecting a original input image with average filtering and there by multiplying with intensity regulated original MR image with in the scale of 49.99-50.01%. The intensities of the pixels on the MR image can be adjusted using the span 10% and 90%.

Step 5: Patches are obtained from converted image by splitting them three times their initial sizes, so that tumours of small size can be enlarged and can be easily detected in the subsequent stages.

Step 6: Multiple threshold values and object counting with erosions help in detecting all possible tumours in each patch.

Step 7: Step 5 and 6 are repeated with the original input MR image till a tumour is identified.

Step 8: Once the tumours are detected during step 5 to step 6. Repeat step 5-7 starting from a transferred index up to pixels of 50 and identified output tumour when it is detached twice during repetition.

Step 9: False tumours are discarded since they are close to the maximum edge of the skull. Fig. 2 gives the flow diagram of the proposed method.

## **IMPLEMENTATION AND RESULTS**

MATlab 2019 environment on core2 Duo processor 1.6 GHz are used. The proposed system is tested and evaluated on the data set available in Brainweb [3, 5]. 20 ground truth MR images were used to detect small size tumours. During testing process multiple early stage tumours along with large size tumours were detected successfully as shown in figure 3(i). At first k-means clustering applied on MR image to cluster the image into three parts. Fig. 3(ii) high intensity region which includes tumour cells, medium intensity region that includes normal tissues and dark regions which does not contain any tissue except skull Figure 3(iii) gives the largest surrounding edge obtained by k-means clusters comprising of bright and medium intensity regions. For both the clusters the boundary outline is achieved using morphological process, which results in identifying the highest neighbouring edge as shown in Fig. 3(iii). Entire amount of pixels in cerebral tissues and other component in skull is obtained by filling gaps in the highest adjoining edge. A value of threshold is arrived based on Euclidean distance on likely tumours obtained from the skullbased pixels. The more the brain size the more proportional the threshold value exist.

In the upcoming stage morphological operations on the original MR Image size applied to identify the tumours. Initially a twofold mask that consists of k-means cluster with intermediate brightness region and largest adjoining edge which is stretched towards the centre by morphological erosion is shown in Fig. 4(i). The enhanced largest edge will be complemented and

multiplied by the intermediate intensity k-means cluster. Fig. 4(ii) shows the major connected component contemplated for gap filling. Next operation gives filtering of original MR image by a minimum averaging filter to remove the noise. The intensity will be adjusted between 49.9% and 50% by multiplying filtrate image by the original

MR image to get the attention on abnormal tissue. The contrast of the resulted image is further adjusted between 10% and 90% to achieve greater concentration on abnormalities. Finally Fig. 4(iii) shows the resultant image after multiplying both modified image.

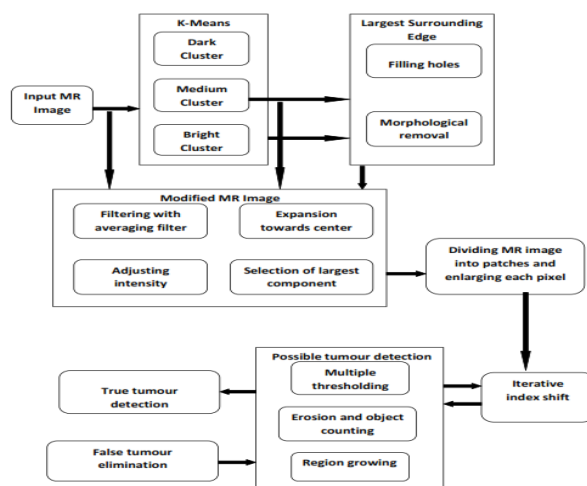


**FIG 2:** Flow diagram of the proposed method for MR image detection and localization technique

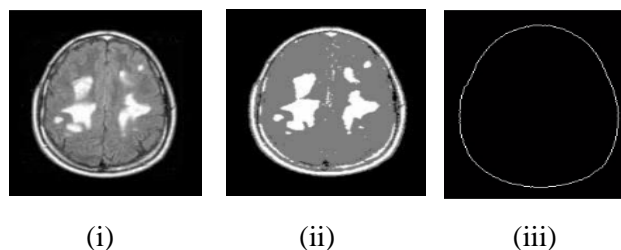


**FIG 3:** Detection of skull edge in MR image using k-means clustering (i) Original Input MR image (ii) clustered MR image (iii) Largest surrounding skull edge

Once modified image is obtained the image is separated into small sections to detect the tumours of minute mass size as shown in figure 4(iv). A single patch will be of size 200 x 200 pixels which will go up to three times larger than the modified image for doing further processing.

Each patch after scaling will be smoothed with an filter having average value followed by morphological operations. For converting a image to binary multiple threshold values of 0.1, 0.3, 0.5, 0.7, 0.9 are used to eliminate small objects [22]. By making use of region growing technique the central point of the resultant binary

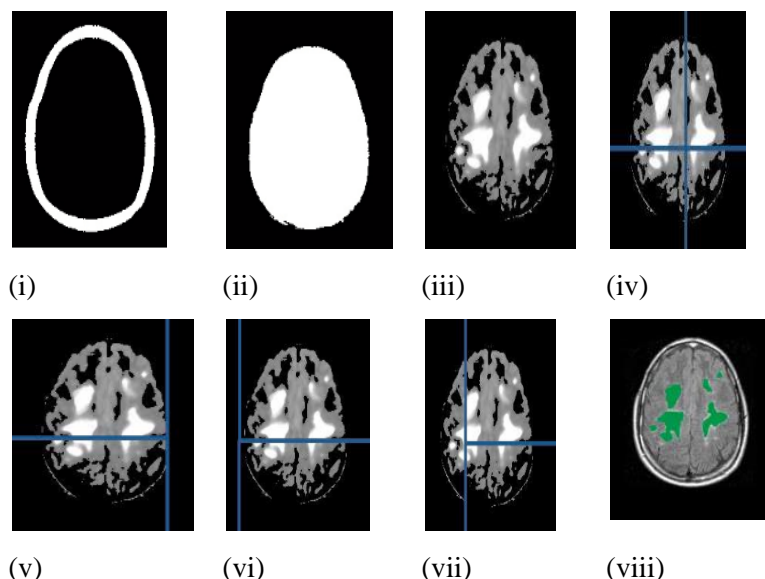
object will be processed till it is equal to one object. The steps are repeated till the intensity is adjusted 35% to 75%, so that the contrast of all the viable tumours will get rid of false dark regions. Finally the resultant tumour is obtained by adding the entire processed image.

Fig. 4(v)-4(vii) shows the entire process which begins with segregate the image into patches will be replicated in steps of 50 pixels. The output of the shifting process produces a pixel value between '0' and '4'. Regions with pixel intensity between '0' and '2' will reflect as possible tumour while others were paid no attention.

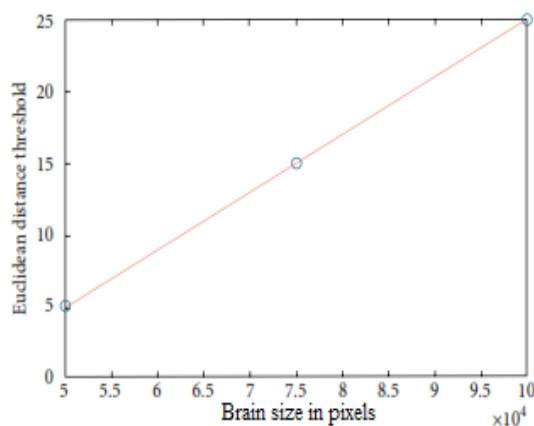
Finally evaluation is done to the detected tumour having tumour or no tumour by hiding Euclidean distance between each detected tumour and largest adjoining edge of the skull.

Figure 4(v)-4(vii) shows the entire process which begins with segregate the image into patches will be replicated in steps of 50 pixels. The output of

the shifting process produces a pixel value between '0' and '4'. Regions with pixel intensity between '0' and '2' will reflect as possible tumour while others were paid no attention. Finally evaluation is done to the detected tumour having tumour or no tumour by hiding Euclidean distance between each detected tumour and largest adjoining edge of the skull.



**FIG 4:** MR image tumour detection using morphological technique (i) highest surrounding edge extended inwards (ii) highest connected component structure (iii) updated MR image (iv) MR image patches (v to vii) patch shifting with different orientation (viii) final tumour detected image



**FIG 5:** Brain size in pixel with respect to Euclidean distance threshold

A tissue will be considered as tumour only whose Euclidean distance from the skull is less than the chosen threshold value which was concluded using the region of the brain image given in Fig. 5. Hence it is clear that Euclidean distance threshold value will be directly proportionate to

the entire amount of pixels in the brain. The threshold values are assigned so that 4 and 5 for smaller brain areas such as 6000 to 9000 pixels and 25 threshold value for larger brain area pixels such as 90,000 to 100000. Fig. 4(viii) gives the detected tumour after tumour evaluation. From

the final results it can be noted that both tiny and large size tumours are detected, while false tumours and skull part are discarded. Fig. 6 shows the 20 MR images of different sizes

containing multiple tumours of both small and large tumors. These images are tested using proposed techniques and achieved promising results.

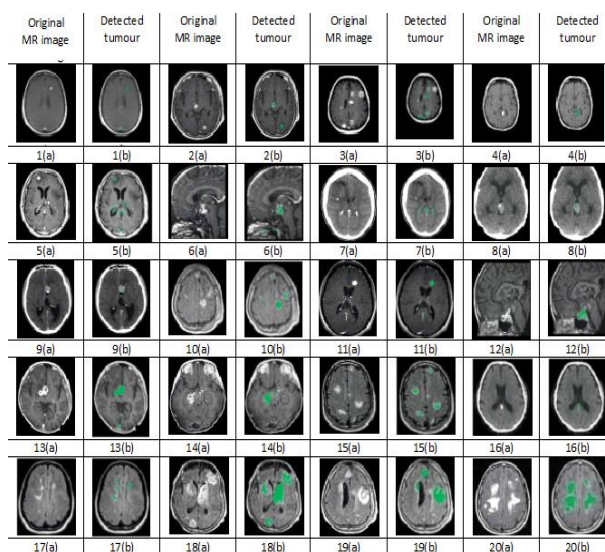


**FIG 6:** Experimental Results of MR brain images (1-20) detecting tumours of dissimilar sizes and intensity levels

**TABLE 1:** Proposed technique performance parameter results

| Test image | Tumour detected pixels | Ground truth pixels | Precision | Sensitivity | Specificity | Dice score coefficient | Accuracy |
|------------|------------------------|---------------------|-----------|-------------|-------------|------------------------|----------|
| 1          | 347                    | 399                 | 1.000     | 0.870       | 1.000       | 0.935                  | 0.999    |
| 2          | 471                    | 570                 | 1.000     | 0.826       | 1.000       | 0.905                  | 0.999    |
| 3          | 397                    | 429                 | 1.000     | 0.925       | 1.000       | 0.961                  | 0.998    |
| 4          | 106                    | 109                 | 1.000     | 0.972       | 1.000       | 0.986                  | 0.999    |
| 5          | 1538                   | 1618                | 1.000     | 0.992       | 1.000       | 0.996                  | 0.999    |
| 6          | 1725                   | 1531                | 1.000     | 0.805       | 0.998       | 0.892                  | 0.996    |
| 7          | 216                    | 239                 | 1.000     | 0.904       | 1.000       | 0.949                  | 0.999    |
| 8          | 61                     | 62                  | 1.000     | 0.984       | 1.000       | 0.992                  | 0.999    |
| 9          | 23                     | 29                  | 1.000     | 0.800       | 1.000       | 0.888                  | 0.999    |
| 10         | 511                    | 520                 | 1.000     | 0.982       | 1.000       | 0.991                  | 0.999    |
| 11         | 1860                   | 2057                | 1.000     | 0.904       | 1.000       | 0.949                  | 0.999    |
| 12         | 2332                   | 2298                | 1.000     | 0.994       | 1.000       | 0.997                  | 0.998    |
| 13         | 4195                   | 4321                | 1.000     | 0.971       | 1.000       | 0.985                  | 0.999    |
| 14         | 3058                   | 3258                | 1.000     | 0.938       | 1.000       | 0.968                  | 0.999    |
| 15         | 519                    | 583                 | 1.000     | 0.890       | 1.000       | 0.941                  | 0.998    |
| 16         | 108                    | 115                 | 1.000     | 0.938       | 1.000       | 0.968                  | 0.999    |
| 17         | 510                    | 592                 | 1.000     | 0.861       | 1.000       | 0.925                  | 0.998    |
| 18         | 2870                   | 3260                | 1.000     | 0.880       | 1.000       | 0.936                  | 0.988    |
| 19         | 1810                   | 2162                | 1.000     | 0.837       | 1.000       | 0.911                  | 0.988    |
| 20         | 2168                   | 2218                | 1.000     | 0.977       | 1.000       | 0.988                  | 0.998    |
| Average    | -                      | -                   | 0.985     | 0.9217      | 0.998       | 0.958                  | 0.998    |

**TABLE 2:** Comparison between existing techniques and proposed technique

| Evaluation parameters  | Existing techniques         |                        |                         | Proposed technique |
|------------------------|-----------------------------|------------------------|-------------------------|--------------------|
|                        | A. Praveen Kumar et al [21] | M. Meshram et al. [19] | K Sooknanan et al. [16] |                    |
| Precision              | -                           | 1.000                  | 0.900                   | 0.9848             |
| Sensitivity            | 0.840                       | 0.9162                 | 0.700                   | 0.9217             |
| Specificity            | -                           | -                      | 1.000                   | 0.9999             |
| Dice score coefficient | -                           | -                      | 0.800                   | 0.9588             |
| Accuracy               | 0.9261                      | 0.896                  | -                       | 0.9989             |

**DISCUSSION**

The proposed method is implemented and tested such that the technique is capable detecting multiple low intensity and large size tumours in MR image. As a sample Figure 6 (18(b)) has eight tumours of different sizes and all eight tumours in sample image have been successfully detected.

The performance metrics used to evaluate the results are precession, sensitivity, and Specificity. Also Dice score coefficient is used to measure the regions overlapped by area segmenting manually and automatically. Finally accuracy is found to evaluate the efficiency of the system as shown in the equation 7.

The performance parameters with regard to MR images given as sample input in figure 6 give a

result in Table 1. The average value for precession, specificity and accuracy are 98.58, 99.91 and 99.98% respectively. The sensitivity average value is 92.16% while the dice score coefficient average value is 95.81%.

According to Table 2, the evaluation of the suggested technique is compared to other ones that are already in use. The best conceivable value for specificity is the average of 99.98%. The sensitivity, on the other hand, is 92.17%, which is significantly higher than the value of 91.62 obtained by M. Meshram et al [19]. Dice-score coefficient is 95.88%, which is significantly higher than the value of 80% that K Sooknanan et al. [16] obtained. The accuracy of 99.89% is also significantly higher than the 92.61 percent reported by A. Praveen Kumar et al. [21].

|  |     |
|--|-----|
| $Precision = \frac{TP}{TP + FP}$                         | (3) |
| $Sensitivity = \frac{TP}{TP + FN}$                       | (4) |
| $Specificity = \frac{TN}{TN + FP}$                       | (5) |
| $Dicescorecoefficient = \frac{2 * TP}{2 * TP + FP + TN}$ | (6) |
| $Accuracy = \frac{TP + TN}{TP + FP + FN + TN}$           | (7) |

**CONCLUSION**

Innovative MR image segmentation plays an important role in the detection and treatment of brain tumour. Early detection of malignant tumours which is in starting stage will allow

doctors decide appropriate treatment and increase the chances of patents survival. In this study, automated tumour detection technique is proposed with localization of earlystage brain tumours using k-means clustering, patch based

processing and object counting. The experimental results for 20 ground truth MR images are able to detect tumours independent of their size, intensity or orientation. To make the technique more vigorous a way to ascertain the type of tumour and its thickness can be explored in the future.

## REFERENCES

1. Dixit, Abhishek, and Pooja Singh. "Brain Tumor Detection Using Fine-Tuned YOLO Model with Transfer Learning." In *Artificial Intelligence on Medical Data*, pp. 363-371. Springer, Singapore, 2023.
2. Lotlikar, Venkatesh S., Nitin Satpute, and Aditya Gupta. "Brain Tumor Detection Using Machine Learning and Deep Learning: A Review." *Current Medical Imaging* 18.6 (2022): 604-622.
3. Bruno, Federico, Vincenza Granata, Flavia Cobianchi Bellisari, Ferruccio Sgalambro, Emanuele Tommasino, Pierpaolo Palumbo, Francesco Arrigoni et al. "Advanced Magnetic Resonance Imaging (MRI) Techniques: Technical Principles and Applications in Nanomedicine." *Cancers* 14, no. 7 (2022): 1626.
4. Chattopadhyay, Arkapravo, and Mausumi Maitra. "MRI-based Brain Tumor Image Detection Using CNN based Deep Learning Method." *Neuroscience Informatics* (2022): 100060.
5. Aaraji, Zahraa Sh., and Hawraa H. Abbas. "Automatic Classification of Alzheimer's Disease using brain MRI data and deep Convolutional Neural Networks." *arXiv preprint arXiv:2204.00068* (2022).
6. Rahman, Jawwad Sami Ur, and Sathish Kumar Selvaperumal. "Integrated approach of brain segmentation using neuro fuzzy k-means." *Indonesian Journal of Electrical Engineering and Computer Science* 29, no. 1 (2023): 270-276.
7. Pei, Linmin, Murat Ak, NourelHoda M. Tahon, Serafettin Zenkin, Safa Alkarawi, Abdallah Kamal, Mahir Yilmaz et al. "A general skull stripping of multiparametric brain MRIs using 3D convolutional neural network." *Scientific Reports* 12, no. 1 (2022): 1-11.
8. Pei, Linmin, A. K. Murat, Nourel Tahon, Serafettin Zenkin, Safa Karawi, Abdallah Kamal, Mahir Yilmaz, Lingling Chen, Mehmet Er, and Rivka Colen. "A Generative Skull Stripping of Multiparametric Brain MRIs Using 3D Convolutional Neural Network." (2022).
9. Duarte, Kauê Tartarotti Nepomuceno, Marina Andrade Nascimento Moura, Paulo Sergio Martins, and Marco Antonio Garcia de Carvalho. "Brain Extraction in Multiple T1-weighted Magnetic Resonance Imaging slices using Digital Image Processing techniques." *IEEE Latin America Transactions* 20, no. 5 (2022): 831-838.
10. D. L. Pham, C. Xu, and J. L. Prince, "Current methods in medical image segmentation," *Annual Review of Biomedical Engineering*, vol. 2, no. 1, pp. 315-337, 2000.
11. S. A. Karkanis, D. K. Iakovidis, D. E. Maroulis, D. A. Karras, and M. Tzivras, "Computer-aided tumor detection in endoscopic video using color wavelet features," *IEEE Transaction on Information Technology in Biomedicine*, vol. 7, no. 3, pp. 141-152, 2003.
12. Grande-Barreto, Jonas, and Pilar Gómez-Gil. "Pseudo-label-assisted self-organizing maps for brain tissue segmentation in magnetic resonance imaging." *Journal of Digital Imaging* 35, no. 2 (2022): 180-192.
13. K. Sinha and G. R. Sinha, "Efficient segmentation methods for tumor detection in MRI images," in *Proceedings of the IEEE International Journal of Biomedical Imaging Students' Conference on Electrical, Electronics and Computer Science*, pp. 1-6, IEEE, Piscataway, NJ, USA, 2014.
14. Y. Megersa and G. Alemu, "Brain tumor detection and segmentation using hybrid intelligent algorithms," in *Proceedings of the AFRICON*, pp. 1-8, IEEE, Piscataway, NJ, USA, 2015.
15. N. B. Bahadure, A. K. Ray, and H. P. Theethi, "Image analysis for MRI based brain tumor detection and feature extraction using biologically inspired BWT and SVM," *International Journal of Biomedical Imaging*, vol. 2017, Article ID 9749108, 12 pages, 2017.
16. Hanuman and K. Sooknanan, "Brain tumor segmentation and volume estimation from T1-contrasted and T2 MRIs," *International Journal of Image Processing (IJIP)*, vol. 12, no. 2, pp. 48-62, 2018.
17. Hazra, A. Dey, and S. K. Gupta, M. A. Ansari, "Brain tumor detection based on segmentation using MATLAB," in *Proceedings of the International Conference on Energy, Communication, Data Analytics and So Computing (ICECDS)*, pp. 425-430, IEEE, Piscataway, NJ, USA, 2017.
18. Kharrat, N. Benamrane, M. B. Messaoud, and M. Abid, "Detection of brain tumor in medical

- images,” in Proceedings of the 3rd International Conference on Signals, Circuits and Systems (SCS), pp. 1–6, IEEE, Piscataway, NJ, USA, 2009.
19. Gujar and C. M. Meshram, “Brain tumor extraction using genetic algorithm,” *International Journal on Future Revolution in Computer Science and Communication engineering (IJFRSCE)*, vol. 4, no. 6, pp. 33–39, 2018.
  20. S. Pereira, A. Pinto, V. Alves, and C. A. Silva, “Brain tumor segmentation using convolutional neural networks in MRI images,” *IEEE Transactions on Medical Imaging*, vol. 35, no. 5, pp. 1240–1251, 2016.
  21. Kullayamma and A. Praveen Kumar, “Brain tumor segmentation by using ant colony optimization,” *International Journal of Scientific Research in Science and Technology*, vol. 4, no. 8, pp. 62–69, 2018.
  22. Boussselham, O. Bouattane, M. Youssefi, and A. Raihani, “Towards reinforced brain tumor segmentation on MRI images based on temperature changes on pathologic area,” *International Journal of Biomedical Imaging*, vol. 2019, Article ID 1758948, 18 pages, 2019.
  23. C. Zhang, X. Shen, H. Cheng, and Q. Qian, “Brain tumor segmentation based on hybrid clustering and morphological operations,” *International Journal of Biomedical Imaging*, vol. 2019, Article ID 7305832, 11 pages, 2019.
  24. S. K. Sahu, M. B. N. V. Prasad, and B. K. Tripathy, “A support vector machine binary classification and image segmentation of remote sensing data of chilikalagoon,” *International Journal of Research in Information Technology*, vol. 3, no. 5, pp. 191–204, 2015.